Fluorescent and Electrochromic Aromatic Polyamides with 4-*tert*-Butyltriphenylamine Chromophore

SHENG-HUEI HSIAO,[1] **GUEY-SHENG LIOU,**[2] **YI-CHUN KUNG,**[3] **YU-MING CHANG**[3]

[1]Department of Chemical Engineering and Biotechnology, National Taipei University of Technology, Taipei 10608, Taiwan

[2]Institute of Polymer Science and Engineering, National Taiwan University, Taipei 10617, Taiwan

[3]Department of Chemical Engineering, Tatung University, Taipei 10451, Taiwan

ABSTRACT: A new triphenylamine-based aromatic dicarboxylic acid monomer, 4-*tert*-butyl-4′,4″-dicarboxytriphenylamine (**2**), was synthesized from the cesium fluoride mediated *N,N*-diarylation reaction of 4-*tert*-butylaniline with 4-fluorobenzonitrile and subsequent alkaline hydrolysis of the dinitrile intermediate. A series of six aromatic polyamides **4a-4f** with *tert*-butyltriphenylamine groups was prepared from the newly synthesized dicarboxylic acid and various aromatic diamines. These polyamides were readily soluble in many organic solvents and could be solution-cast into flexible and strong films. The glass-transition temperatures of these polymers were in the range of 274–311 °C. These polymers exhibited strong UV-vis absorption bands at 356–366 nm in NMP solution. Their photoluminescence spectra showed maximum bands around 433–466 nm in the blue region. Cyclic voltammograms of all the polyamides exhibited reversible oxidation redox couples in acetonitrile. The polyamide **4f,** with *tert*-butyltriphenylamine segment in both diacid and diamine residues, exhibited stable electrochromic characteristics with a color change from a colorless neutral form, through a green semioxidized form, to a deep purple fully oxidized form. © 2010 Wiley Periodicals, Inc. J Polym Sci Part A: Polym Chem 48: 2798–2809, 2010

KEYWORDS: cyclic voltammetry; electrochemistry; electrochromism; fluorescence; polyamides; spectroelectrochemistry; triphenylamine

INTRODUCTION Triarylamines are an important class of aromatics because they are easily oxidized to form stable aminium cation radicals. In view of their stability, triarylamine cation radicals have become promising spin-containing units for exploitation of potential organic magnetic materials.[1–5] Perhaps most commonly, triarylamine derivatives have been used as the hole-transport and/or light-emitting materials in electroluminscent devices.[6–10] Most of triarylamine derivatives are used as vapor-deposited thin films, or composite materials dispersed in an inert polymer binder. It is, however, difficult to maintain long-term morphological stability due to crystallization or phase separation. One of the methods to overcome this drawback could be the incorporation of triarylamine units into the polymer backbone or into its side chains.[11–15] The extensive investigations on the polymeric materials have shown the possibility of enhancing the device performance due to the increased morphological stability.[16–20] In addition, the uses of polymeric materials exhibit another advantages, such as good processability and variety of possible chemical modification.[21–26]

Wholly aromatic polyamides are characterized as highly thermally stable polymers with a favorable balance of physical and chemical properties. However, rigidity of the backbone and strong hydrogen bonding results in high melting or glass-transition temperatures (T_gs) and limited solubility in most organic solvents.[27,28] These properties make them generally intractable or difficult to process, thus restricting their applications. To overcome such a difficulty, polymer structure modification becomes necessary. It has been reported that aromatic polyamides bearing the propeller-shaped triphenylamine (TPA) unit in the main chain were amorphous and easily soluble in organic solvents and they could be solution-cast into flexible films with good mechanical property and high thermal stability.[29–31] In recent years, we have demonstrated that TPA-based polymers are promising hole-transporting and electrochromic materials for optoelectronic applications due to the electroactive TPA units.[32–42] It has also been reported in our previous publications[36,41,42] that the incorporation of electron-donating substituents such as *tert*-butyl and methoxy groups on the electrochemically active sites of the TPA unit resulted in stable TPA cationic radicals and decreased oxidation potential, leading to a significantly enhanced redox and electrochromic stability of the prepared polyamides. In an effort to extend our work to the design and synthesis of electrochromic high-performance polymers, herein we wish to synthesize a new

tert-butyl-substituted TPA-based dicarboxylic acid, namely 4-*tert*-butyl-4′,4″-dicarboxytriphenylamine, and its derived aromatic polyamides. The optoelectronic and fluorescence properties of the prepared polymers were also investigated. As compared to the corresponding counterparts derived from 4,4′-diamino-4″-*tert*-butyltriphenylamine and aromatic dicarboxylic acids we reported previously,[34] the present polyamides exhibited a slightly higher oxidation potential, but with a stronger fluorescence intensity and different coloration changes upon electrochemical oxidation.

EXPERIMENTAL

Materials

4-*tert*-Butylaniline (Acros), 4-fluorobenzonitrile (TCI), sodium hydride (NaH; Fluka), and triphenyl phosphite (TPP, Acros) were used without further purification. *N,N*-Dimethylacetamide (DMAc, Fluka), *N,N*-dimethylformamide (DMF, Acros), pyridine (Py, Wako), and *N*-methyl-2-pyrrolidone (NMP, Fluka) were dried over calcium hydride for 24 h, distilled under reduced pressure, and stored over 4 Å molecular sieves in a sealed bottle. According to the previously reported procedures,[43] the CF$_3$-containing diamine, 2-trifluoromethyl-4,4′-diaminodiphenyl ether (**3d**) (mp = 112–113 °C), was prepared from the chloro-displacement reaction of 2-chloro-5-nitrobenzotrifluoride with 4-nitrophenol in the presence of potassium carbonate, followed by Pd/C-catalyzed hydrazine reduction. 4,4′-Diamino-4″-*tert*-butyltriphenylamine (**3f**) (mp = 113–115 °C) was prepared by the cesium fluoride-mediated aromatic nucleophilic substitution reaction of 4-fluoronitrobenzene with the 4-*tert*-butylaniline followed by Pd/C-catalyzed hydrazine reduction, as described in one of our previous publications.[34] Commercially available aromatic diamines such as *p*-phenylenediamine (**3a**, TCI), *m*-phenylenediamine (**3b**, Acros), 4,4′-diaminophenyl ether (**3c**, TCI), and 9,9-bis(4-aminophenyl)fluorene (**3e**, TCI) were used as received. Commercially obtained calcium chloride was dried under vacuum at 150 °C for 6 h before use. Tetrabutylammonium perchlorate (TBAP, TCI) was recrystallized twice from ethyl acetate and then dried in vacuum before use.

Monomer Synthesis

4-Tert-*butyl*-4′,4″-*dicyanotriphenylamine (1)*

A mixture of 4.0 g (0.1 mol) of 60% sodium hydride in 80 mL of dry DMSO was stirred at room temperature. To the mixture, 7.46 g (0.05 mol) of 4-*tert*-butylaniline and 12.1 g (0.1 mol) of 4-fluorobenzonitrile were slowly added in sequence. The mixture was heated with stirring at 120 °C for 12 h. After cooling, the mixture was poured into 300 mL of aqueous sodium chloride solution, and the sticky product gradually solidified after being soaked in ethanol. Recrystallization from ethanol yielded 9.3 g (53% yield) of pure dinitrile compound **1** as yellow crystals [mp = 188–189 °C, measured by differential scanning calorimetry (DSC) at a scan rate of 2 °C/min]. IR (KBr): 2217 cm^{-1} (-C≡N stretch).

^{1}H NMR (500 MHz, CDCl$_3$, δ, ppm): 7.51 (d, *J* = 8.6 Hz, 4H, H$_d$), 7.40 (d, *J* = 8.5 Hz, 2H, H$_a$), 7.11 (d, *J* = 8.6 Hz, 4H, H$_c$), 7.05 (d, *J* = 8.5 Hz, 2H, H$_b$), 1.28 (s, 9H, *tert*-butyl). ^{13}C NMR

(125 MHz, CDCl$_3$, δ, ppm): 150.7 (C^7), 150.2 (C^6), 142.6 (C^3), 133.9 (C^9), 127.6 (C^4), 127.0 (C^5), 123.1 (C^8), 119.4 (-CN), 105.9 (C^{10}), 35.1 (C^2), 31.8 (C^1). Crystal data for **1**: yellow single crystal grew by the slow crystallization from ethanol, crystal dimensions: 0.5 × 0.4 × 0.3 mm^3, Monoclinic, space group P 21/a, *a* = 12.3393(4) Å, *b* = 13.3826(4) Å, *c* = 12.4031(5) Å, α = 90°, β = 97.8470° (10), γ = 90°, *D*$_{calcd}$ = 1.150 mg/m^3, *Z* = 4, and *V* = 2028.97(12) Å^3.
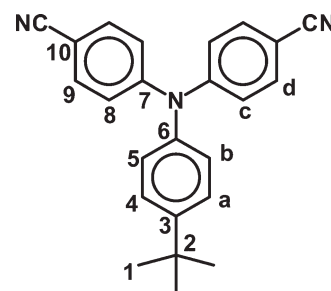

4-Tert-*butyl*-4′,4″-*dicarboxytriphenylamine (2)*

A mixture of 9.56 g of potassium hydroxide and 5.0 g of the obtained dinitrile compound **1** in 50 mL of ethanol and 50 mL of distillated water was refluxed at 100 °C until no further ammonia was generated. The time taken to reach this stage was about 3 days. The solution was cooled, and the pH value was adjusted by conc. hydrochloric acid (12 M) to near 3. The white precipitate formed was collected by filtration, washed thoroughly with water, and dried *in vacuo* to give 4.6 g (yield = 83%) of diacid **2** (mp = 292–294 °C by DSC at 2 °C/min). IR (KBr): 1686 cm^{-1} (C=O stretch), 2700–3400 cm^{-1} (O—H).

^{1}H NMR (500 MHz, DMSO-*d*$_6$, δ, ppm): 7.85 (d, *J* = 8.6 Hz, 4H, H$_d$), 7.42 (d, *J* = 8.5 Hz, 2H, H$_a$), 7.07 (d, *J* = 8.5 Hz, 2H, H$_b$), 7.04 (d, *J* = 8.6 Hz, 4H, H$_c$), 1.28 (s, 9H, *tert*-butyl). ^{13}C NMR (125 MHz, DMSO-*d*$_6$, δ, ppm): 166.8 (C=O), 150.3 (C^7), 147.9 (C^6), 142.9 (C^3), 130.9 (C^9), 129.1 (C^4), 126.8 (C^5), 126.0 (C^{10}), 122.9 (C^8), 34.2 (C^2), 31.0 (C^1).
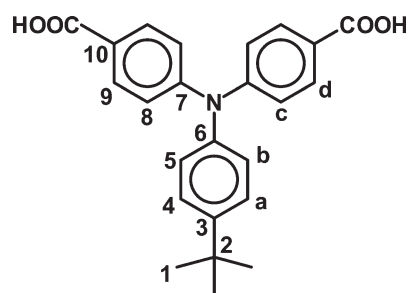
Synthesis of Polyamides

The synthesis of polyamide **4a** is used as an example to illustrate the general synthetic route used to produce the polyamides. A 50 mL round-bottom flask equipped with a
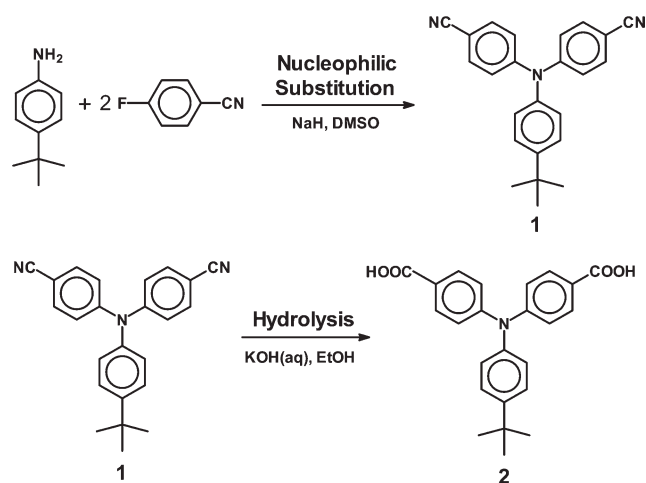
SCHEME 1 Synthetic route to the target dicarboxylic acid monomer **2**.

magnetic stirrer was charged with 0.3895 g (1.00 mmol) of diacid **2**, 0.1081 g (1.00 mmol) of *p*-phenylenediamine (**3a**), 1 mL of TPP, 2 mL of NMP, 0.5 mL of pyridine, and 0.2 g of calcium chloride (CaCl$_2$). The reaction mixture was heated with stirring at 120 °C for 3 h. The polymer solution was poured slowly into 200 mL of stirring methanol giving rise to a stringy, fiber-like precipitate that was collected by filtration, washed thoroughly with hot water and methanol, and dried. The other polyamides were prepared by an analogous procedure. IR (film): 3315 cm^{-1} (amide N—H stretch), 1649 cm^{-1} (amide C=O stretch), 2962 cm^{-1} (*tert*-butyl C-H stretch).

Preparation of the Polyamide Films

A polymer solution was made by the dissolution of about 0.5 g of the polyamide sample in 10 mL of hot DMAc. The homogeneous solution was poured into a 9-cm glass Petri dish, which was placed in a 90 °C oven overnight for the slow release of the solvent, and then the film was stripped off from the glass substrate and further dried in vacuum at 160 °C for 6 h. The obtained films were about 0.08 μm thick and were used for X-ray diffraction measurements, tensile tests, solubility tests, and thermal analyses.

Measurements

Infrared spectra were recorded on a Horiba FT-720 FTIR spectrometer. Elemental analyses were run in a Perkin–Elmer 2400 CHN analyzer. ^{1}H and ^{13}C NMR spectra were measured on a Bruker AVANCE 500 FT-NMR system. The inherent viscosities were determined with a Cannon-Fenske viscometer at 30 °C. Wide-angle X-ray diffraction (WAXD) measurements were performed at room temperature (~25 °C) on a Shimadzu XRD-6000 X-ray diffractometer (40 kV, 30 mA), using nickel-filtered Cu-Kα radiation (λ = 1.5418 Å). The scanning rate was 2 °/min over a range of 2θ = 10–40°. A universal tester LLOYD LRX with a load cell 5 kg was used to study the stress-strain behavior of the samples. A gauge length of 2 cm and a crosshead speed of 5 mm/min were used for this study. Measurements were performed at room temperature with film specimens (0.5 cm width, 6 cm length), and an average of at least three individual determinations was reported. Thermogravimentric analysis (TGA) was conducted with a Perkin–Elmer Pyris 1 TGA. Experiments were carried out on approximately 3–5 mg of samples heated in flowing nitrogen or air (gas flow rate = 40 cm^3/min) at a heating rate of 20 °C/min. DSC analyses were performed on a Perkin–Elmer Pyris 1 DSC at a scan rate of 20 °C/min in flowing nitrogen. Thermomechanical analysis (TMA) was conducted with a Perkin–Elmer TMA 7 instrument. The TMA experiments were conducted from 50 to 350 °C at a scan rate of 10 °C/min with a penetration probe 1.0 mm in diameter under an applied constant load of 10 mN. Softening temperatures (T_s) were taken as the onset temperatures of probe displacement on the TMA traces. Ultraviolet-visible (UV-Vis) spectra of the polymer films were recorded on an Agilent 8453 UV-Visible spectrophotometer. Electrochemistry was performed with a CH Instruments 611C electrochemical analyzer. Voltammograms are presented with the positive potential pointing to the left and with increasing anodic currents pointing downwards. Cyclic voltammetry was conducted with the use of a three-electrode cell in which ITO (polymer films area ca. 0.8 cm ×1.25 cm) was used as a working electrode. A platinum wire was used as an auxiliary electrode. All cell potentials were taken with the use of a homemade Ag/AgCl, KCl (sat.) reference electrode. Ferrocene was used as an external reference calibration (+0.44 V vs. Ag/AgCl). Spectroelectrochemistry analyses were carried out with an electrolytic cell whcih was composed of a 1 cm cuvette, ITO as a working electrode, a platinum wire as an auxiliary electrode, and a Ag/AgCl reference electrode. Absorption spectra in the spectroelectrochemical experiments were measured with an Agilent 8453 UV-Visible diode array spectrophotometer. Photoluminescence (PL) spectra were measured with a Varian Cary Eclipse fluorescence spectrophotometer.

RESULTS AND DISCUSSION

Monomer Synthesis

As depicted in Scheme 1, the new aromatic dicarboxylic acid **2** was successfully synthesized by the alkaline hydrolysis reaction of the dinitrile compound **1**, which was obtained from the condensation reaction of 4-*tert*-butylaniline with 4-fluorobenzonitrile in DMSO in the presence of sodium hydride. IR, ^{1}H NMR and ^{13}C NMR spectroscopic techniques were used to identify the structures of the intermediate dinitrile compound **1** and the targeted dicarboxylic acid monomer **2**. The IR spectrum (see Supporting Information Fig. S1) of dinitrile compound **1** gave a characteristic absorption peak at 2217 cm^{-1} (C≡N stretching). After hydrolysis, the characteristic absorption of the cyano group disappeared, and the carboxylic acid group showed a typical carbonyl absorption band at 1686 cm^{-1} (C=O stretching) together with the appearance of broad bands around 2700–3400 cm^{-1} (O—H stretching). The structures of **1** and **2** were also confirmed by high-resolution NMR spectra. The ^{1}H and ^{13}C NMR spectra of these compounds are illustrated in Figures 1
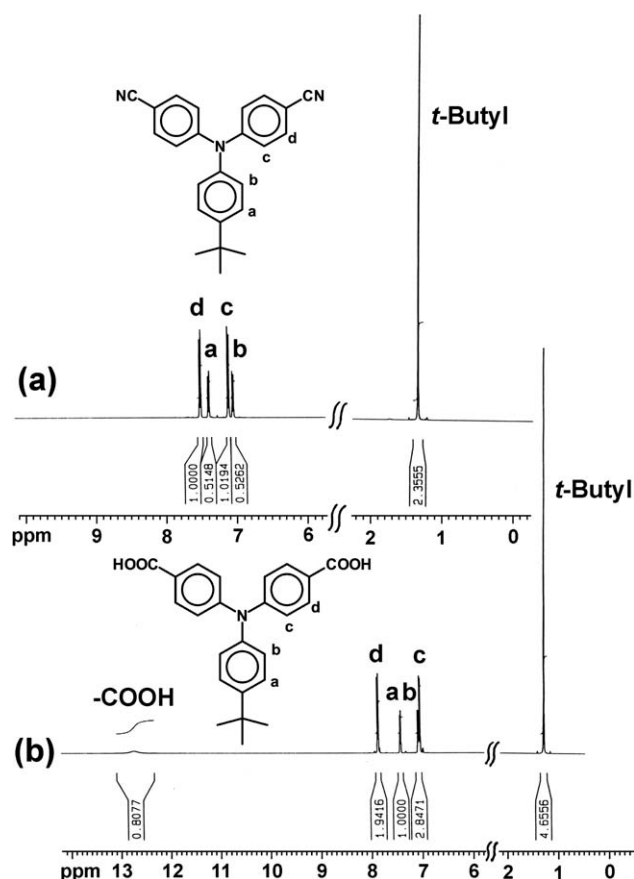
FIGURE 1 ^{1}H NMR spectra of (a) dinitrile compound **1** and (b) dicarboxylic acid monomer **2** in DMSO-d_6.

and 2, respectively. The assignments of each carbon and proton also are given in the figures, and these spectra are in good agreement with the proposed molecular structures. The ^{13}C NMR spectra confirm that the cyano groups were completely converted into the carboxyl groups by the disappearance of the resonance peak for the cyano carbon at 119.4 ppm and the appearance of the carbonyl peak at 166.8 ppm. The signals appeared at 1.28 ppm in the ^{1}H NMR spectrum and 34.2 ppm (a quaternary carbon) and 31.0 ppm (a methyl carbon) in the ^{13}C NMR spectrum are assigned to the *tert*-butyl groups. The molecular structure of **1** was further determined by single-crystal crystallographic analysis (Fig. 3), and the bond length and angle data are summarized in Supporting Information Table S1. As shown in Figure 3, compound **1** displays a propeller-like geometry of the TPA core. This three-dimensional structure together with the bulky *tert*-butyl group will hinder the close packing of polymer chain and enhance the solubility of formed polyamides.

Polymer Synthesis

A series of new aromatic polyamides, **4a–4f**, were prepared from diacid **2** and six aromatic diamines (**3a–3f**) by the Yamazaki-Higashi polyamidation reaction[44] using TPP and pyridine as condensing agents (Scheme 2). All the polymerizations proceeded homogeneously throughout the reaction and afforded clear, highly viscous polymer solutions. These polymers precipitated in a tough, fiber-like form when the resulting polymer solutions were slowly poured into methanol with stirring. These polyamides were obtained in almost quantitative yields, with inherent viscosity in the range of 0.55–0.90 dL/g (Table 1). All the polymers could be solution-cast into flexible and tough films, and this was indicative of the formation of high molecular weight polymers. The IR spectrum of the polyamide **4a** shown in Supporting Information Figure S2 exhibited the characteristic amide absorptions near 3300 and 1650 cm^{-1}, sustaining the formation of the amide linkages. The ^{1}H and ^{13}C NMR of the representative polyamide **4a** agree well with the desired structure (Fig. 4).
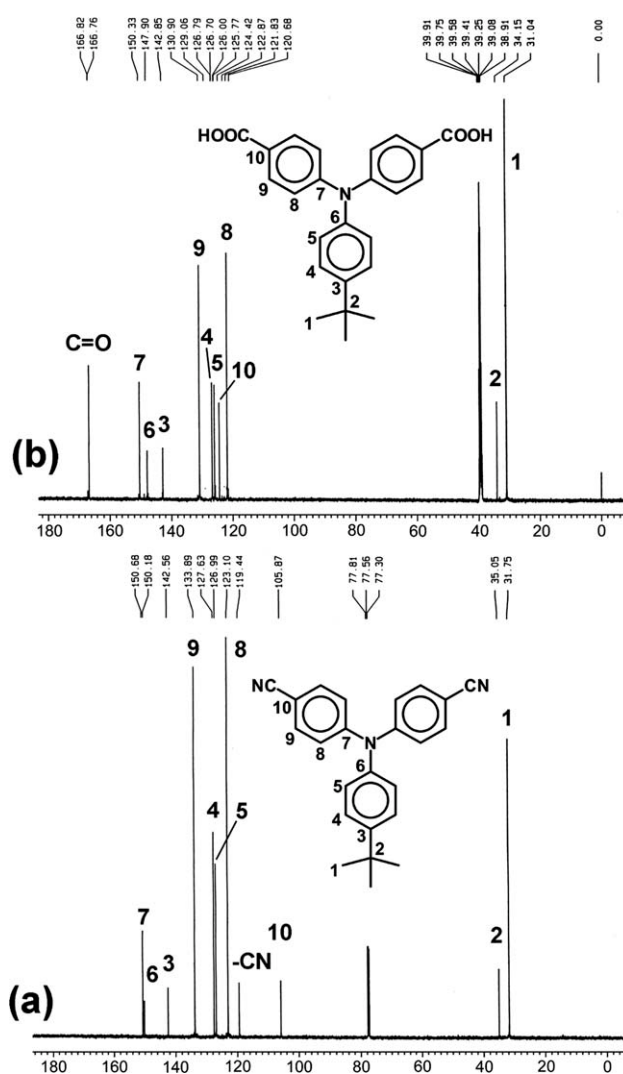
FIGURE 2 (a) ^{13}C NMR spectrum of compound **1** in CDCl$_3$. (b) ^{13}C NMR spectrum of 4-*tert*-butyl-4′,4″-dicarboxytriphenylamine (**2**) in DMSO-d_6.
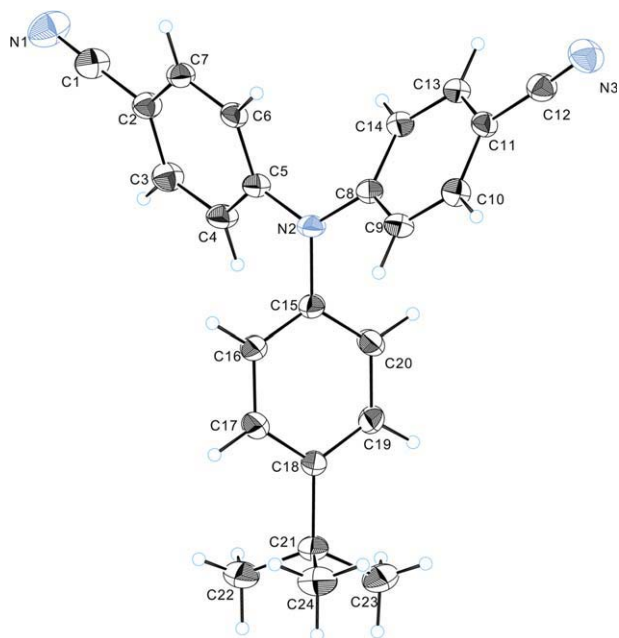
FIGURE 3 Molecular structure of dicyano compound **1** by single crystal X-ray analysis. [Color figure can be viewed in the online issue, which is available at www.interscience.wiley.com.]

Polymer Properties

Organo-Solubility and Film Property

The solubility properties of the polyamides in several organic solvents at 10% (w/v) are also reported in Table 1. All the polymers exhibited good solubility in a variety of dipolar solvents such as NMP, DMAc, *N,N*-dimethylformamide (DMF),

and dimethyl sulfoxide (DMSO) at room temperature or upon heating at 80 °C. They were also soluble in phenol-type solvents such as *m*-cresol; however, they were insoluble in less polar solvents like THF. From the diffraction patterns shown in Supporting Information Figure S3, the X-ray diffraction studies of the polyamides indicated that all the polymers are essentially amorphous. The excellent solubility and amorphous nature of these polyamides can be attributed to the increased free volume caused by the introduction of the three-dimensional TPA moiety and bulky pendent *tert*-butyl substituents into the backbone. Thus, the excellent solubility makes these polymers as potential candidates for practical applications by low-cost spin-coating or inkjet-printing processes. The mechanical properties of the polymer films are summarized in Supporting Information Table S2. They had a tensile strength of 85–97 MPa, an elongation at break of 7–10%, and a tensile modulus of 2.1–2.6 GPa, indicating strong and tough polymeric materials.

Thermal Properties

The thermal properties of the polyamides were investigated by TGA, DSC and TMA. The results are summarized in Table 2. The glass-transition temperatures (T_g) of all the **4** series polymers were observed in the range 274–311 °C by DSC. Polyamide **4e** showed the highest T_g due to the presence of rigid 9,9-diphenylfluorene unit. The softening temperatures (T_s) of the polymer film samples were determined by the TMA method with a loaded penetration probe. They were obtained from the onset temperature of the probe displacement on the TMA trace. A typical TMA trace of polyamide **4a** is illustrated in Figure 5. In almost all cases, the T_s values obtained by TMA are comparable to the T_g values measured
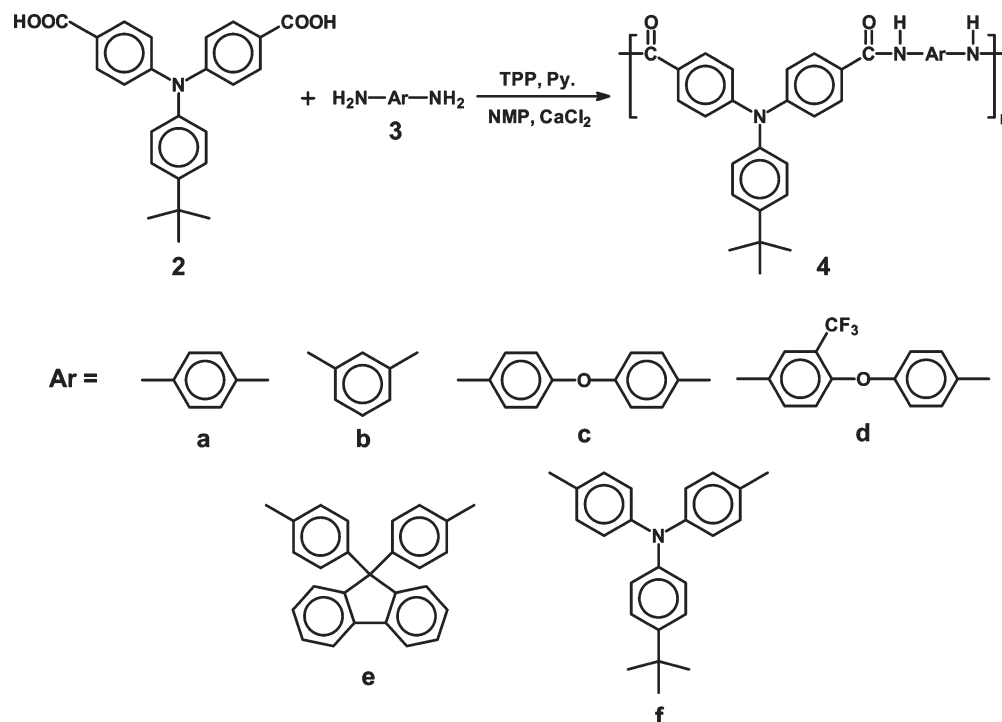
SCHEME 2 Synthesis of polyamides.

TABLE 1 Inherent Viscosity and Solubility Behavior of Polyamides

Polymer Code	η_{inh} (dL/g)[a]	Solubility in Various Solvents[b]					
		NMP	DMAc	DMF	DMSO	*m*-Cresol	THF
4a	0.74	++	++	++	++	++	−
4b	0.57	++	++	++	++	++	−
4c	0.90	++	++	++	++	++	−
4d	0.64	++	++	++	++	++	−
4e	0.69	++	++	++	++	++	−
4f	0.55	++	++	++	++	++	−

++: soluble at room temperature; +: soluble on heating at 80 °C or boiling temperature; −: insoluble even on heating.
[a] Inherent viscosity measured at a concentration of 0.5 g/dL in DMAc −5 wt % LiCl at 30 °C.

[b] Qualitative solubility was determined by using 10 mg sample in 1 mL of stirred solvent. NMP = *N*-methyl-2-pyrrolidone; DMAc = *N*,*N*-dimethylacetamide; DMF = *N*,*N*-dimethylformamide; DMSO = dimethyl sulfoxide; THF = tetrahydrofuran.

by the DSC experiments. Typical TGA thermograms for polyamide **4a** are also included in Figure 5. All of the polymers exhibited reasonable thermal stability. They started to decompose around or above 460 °C and lost 10% weight between 469∼520 °C and 475∼543 °C in nitrogen and air atmosphere, respectively. These polymers afforded high anaerobic char yield in the range of 63–67% at 800 °C in a nitrogen atmosphere. It implied that these polymers still showed good thermal stability irrespective of introducing *tert*-butyl groups in the polymer side chain. For comparison, the thermal behavior data of analogous polyamide **4′** on the basis of 4,4′-dicarboxytriphenylamine are also listed in Table 2. Except for **4b**, the **4** series polyamides showed a slightly decreased T_g as compared to the corresponding **4′** series polyamides. This may be accounted for the increased free volume caused by the introduction of the bulky *tert*-butyl group in the repeat unit. The **4** series polyamides also revealed a slightly decreased thermal stability than the corresponding **4′** analogs. This is reasonable in consideration of the presence of less stable aliphatic segment (*tert*-butyl group).

Absorption and Fluorescence Properties

The optical properties of these polymers were investigated by UV-vis absorption and photoluminescence (PL) spectroscopy. The results are summarized in Table 3. Figure 6 shows the UV-vis absorption and PL emission profiles of four selected polyamides. All the polyamides exhibited strong UV-vis absorption bands at 356–366 nm in NMP solution, assignable to the $\pi-\pi^*$ transitions. Their PL spectra in NMP solution showed maximum bands around 432–498 nm corresponding to blue color (see Fig. 7), with quantum yields (Φ_{PL}) of 0.2–16.5% relative to the quinine sulfate standard (assuming Φ_{PL} = 54.6%).[45] The highest fluorescence quantum yield of 16.5% was observed for polyamide **4e** due to the bulky, rigid 9,9-diphenylfluorene moiety. A relatively higher quantum yield of polyamide **4d** (Φ_{PL} = 15.6%) in comparison to structurally similar **4c** (Φ_{PL} = 5.1%) can be rationalized by the fact that the bulky trifluoromethyl (—CF₃) group decreased the rotational freedom of the ether linkage and its presence might effectively reduce charge transfer formation within or between polymer chains

through steric hindrance and inductive effect (by decreasing the electron-donating character of diamine moieties). The significantly decreased quantum efficiency (Φ_{PL} = 1.4%) of polyamide **4a** when compared with polyamide **4b** (Φ_{PL} = 12.9%) seems to indicate possible charge-transfer quenching effect exerting in the former due to the *p*-phenylenediamine residue. In comparison to the corresponding counterparts derived from 4,4′-diamino-4″-*tert*-butyltriphenylamine (i.e., diamine **3f**) and aromatic dicarboxylic acids we reported earlier,[34] the present polyamides exhibited a stronger fluorescence intensity. This may be rationalized by the fact that the TPA structure is inserted between the carboxyl functionalities for the present polyamides. This possibly decreases the nonradiative charge-transfer interactions between the diamine residue (donor) and the benzoyl unit (acceptor). The very low Φ_{PL} value (0.2%) associated with polyamide **4f** possibly could be attributed to the fact that its excited-state energy is more likely released by vibrational relaxation because of the greater conformational mobility. The polymer
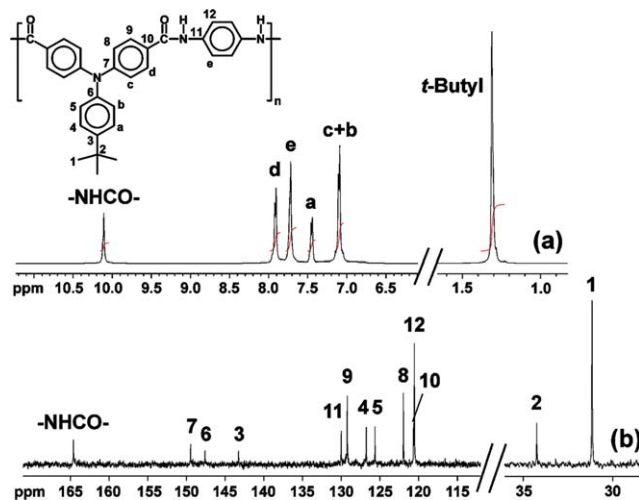
FIGURE 4 (a) ^{1}H NMR and (b) ^{13}C NMR spectra of polyamide **4a** in DMSO-d_6. [Color figure can be viewed in the online issue, which is available at www.interscience.wiley.com.]

TABLE 2 Thermal Properties of Polyamides[a]

| Polymer Code	T_g (°C)[b]	T_s (°C)[c]	T_d (°C)[d] In N_2	In Air	Char Yield (wt %)[e]
4a	288	287	484	478	67
4b	286	284	484	502	67
4c	274	269	469	489	65
4d	281	274	478	475	63
4e	311	316	520	543	63
4f	303	298	510	511	64
4'a	293	288	496	513	70
4'b	271	270	505	512	74
4'c	280	277	495	496	67
4'e	316	318	538	540	66

[a] The polymer film sample were heated at 300 °C for 1 h before all the thermal analyses.
[b] Midpoint temperature of baseline shift on the heating DSC trace (from 50 to 400 °C at 20 °C/min).
[c] Softening temperature taken as the onset temperature of the probe displacement on the TMA trace at a heating rate of 10 °C/min.
[d] Decomposition temperature at which a 10 wt % loss was recorded by TGA at a heating rate of 20 °C/min and a gas flow rate of 40 cm^3/min.
[e] Residual weight percentages at 800 °C in nitrogen.
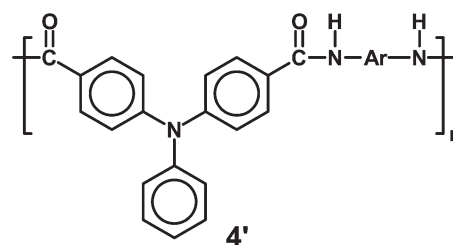
4'

Electrochemical Properties

The redox behavior of these polyamides was investigated by cyclic voltammetry (CV) for the cast films on an ITO-coated glass substrate as working electrode in 0.1 M TBAP/acetonitrile (CH_3CN) solution. The redox potentials of the polyamides as well as their highest occupied molecular orbital (HOMO) and lowest unoccupied molecular orbital (LUMO) energy levels (below vacuum) are also listed in Table 3. Figure 8(b) depicts the CV curve of polyamide **4e**, which was representative for the other polyamides **4a** to **4d**. Polyamide **4e** exhibited a single and well-defined reversible redox couple, with oxidation half-wave potential ($E_{1/2}$) at 1.14 V versus Ag/AgCl, when the potential was scanned between 0.0 and 1.4 V. We noted that the color of polyamide **4e** film changed from colorless to pale blue upon oxidation. Polyamides **4a-4d** showed very similar CV curves to that of **4e,** with $E_{1/2}$ values ranging from 1.15 to 1.18 V. It is noteworthy to mention that changing the diamine structure did not significantly affect the oxidation of the TPA cores of polymers **4a-4e**. It is also can be seen that the oxidation of polyamides **4a-4e** is less facile than that of analogues based on 4,4'-diamino-4''-*tert*-butyltriphenylamine ($E_{1/2}$ = 0.80–0.85 V)[34] owing to the electron-withdrawing effect of the remaining carbonyl groups that destabilize the cationic radi-

cal species. Nevertheless, CV measurements show that polymers **4a-4e** undergo a reversible process, reflecting high oxidation stability, due to the substitution of *tert*-butyl group. For the **4'** series polyamides (see Table 3), they generally possessed an irreversible redox behavior in the anodic oxidative scanning. Thus, the good elelctrochemical redox reversibility for the **4** series polymers confirms that *para*-substitution of the *tert*-butyl group on the TPA unit results in an enhanced stability to the radical cation species. In general, the present series polyamides revealed a similar redox stability to that of the methoxy-substituted analogs reported previously.[35]

As can be seen from Figure 8(c), polyamide **4f** exhibits two redox amino centers in each repeat unit and shows two corresponding well-defined, quasi-reversible anodic redox couples. The first oxidation at $E_{1/2}$ = 0.85 V appears to involve one electron loss from the TPA unit in the diamine residue, and the second oxidation wave ($E_{1/2}$ = 1.27 V) is related to the electron loss from the TPA unit in the diacid residue. In fact, the first oxidation potential is found to be similar to those of polyamides derived from diamine **3f** and conventional aromatic dicarboxylic acids.[34] A clear coloration change was also observed for the film of **4f** upon oxidation, from colorless to green and then to purple.

The external ferrocene/ferrocenium (Fc/Fc$^+$) rodox standard has $E_{1/2}$ at 0.44 V versus Ag/AgCl in acetonitrile. Under the assumption that the HOMO level for the ferrocene standard was 4.80 eV with respective to the zero vacuum level, the
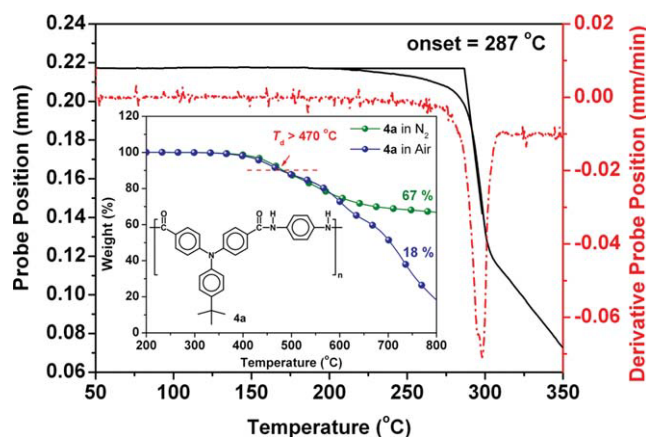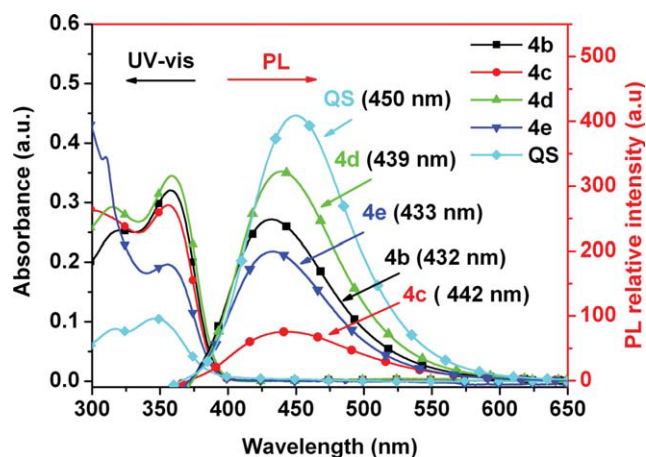
FIGURE 5 TMA and TGA curves of polyamide **4a** with a heating 10 and 20 °C/min, respectively. [Color figure can be viewed in the online issue, which is available at www.interscience.wiley.com.]

FIGURE 6 UV-vis absorption and PL spectra of polyamides **4b**, **4c**, **4d**, and **4e** with a concentration of 1×10^{-5} M in NMP. Quinine sulfate dissolved in 1N $H_2SO_{4(aq)}$ (1×10^{-5} M) as the standard ($\Phi_F = 54.6\%$). Data indicated in parentheses are the emission maximum of the PL spectra. [Color figure can be viewed in the online issue, which is available at www.interscience.wiley.com.]

HOMO levels for the **4** series polyamides were estimated to be 4.99–5.40 eV calculated from the onset oxidation potentials (E_{onset}). These data together with absorption spectra were then used to obtain the LUMO energy levels. These polyamides have good hole-injection and hole-transporting ability, because their HOMOs are close to the common hole-injection materials such as PEDOT:PSS ($\sim$5.2 eV).[46]

Spectroelectrochemical and Electrochromic Properties

Following the electrochemical tests, the optical properties of the electrochromic films were evaluated by using spectroelectrochemistry at different applied potentials. The electrode

preparations and solution conditions were identical to those used in CV. The polymers were drop-coated as films on ITO/glass substrates and mounted in a spectroelectrochemical cell. The typical absorption spectral changes of polyamide **4e** (representative for the **4a–4e** series) are shown in Figure 9. The oxidation of **4e** started to occur at 1.10 V. When the applied potential was gradually increased from 1.10 to 1.35 V, the absorbption band at 360 nm decreased and a

TABLE 3 Optical and Electrochemical Properties of Polyamides

Code	Abs λ_{max} (nm)[a]	Abs λ_{onset} (nm)[b]	PL λ_{max} (nm)[c]	Φ_{PL} (%)[d]	Oxidation Potential (V)[e] $E_{1/2}$ 1st	2nd	E_{onset}	E_g^{opt} (eV)[f]	$E_{HOMO/LUMO}$ (eV)[g]
4a	364 (370)	413	458	1.4	1.18	–	1.00	3.00	5.36/2.36
4b	358 (364)	410	432	12.9	1.15	–	1.01	3.02	5.37/2.35
4c	356 (358)	406	442	5.1	1.17	–	1.03	3.05	5.39/2.34
4d	358 (365)	411	439	15.6	1.16	–	1.03	3.02	5.39/2.37
4e	356 (363)	416	433	16.5	1.14	–	1.04	2.98	5.40/2.42
4f	366 (368)	432	498	0.2	0.85	1.27	0.63	2.87	4.99/2.12
4′a	365 (361)	408	421	1.2	(1.18)[h]	–	1.02	3.03	5.38/2.35
4′b	356 (361)	405	421	9.6	(1.16)[h]	–	1.02	3.06	5.38/2.32
4′c	355 (361)	414	419	3.8	(1.19)[h]	–	1.03	3.00	5.39/2.39
4′e	355 (360)	412	423	11.5	1.15	–	1.02	3.01	5.38/2.37

[a] UV/vis absorption measured in NMP (10^{-5} M) at room temperature. Data shown in parentheses are those measured as thin solid-film.
[b] Absorption edge (λ_{onset}) measured in thin solid-film at room temperature.
[c] PL spectra measured in NMP (10^{-5} M) at room temperature.
[d] The quantum yield was measured by using quinine sulfate (dissolved in 1 N H_2SO_4 with a concentration of 1×10^{-5} M, assuming photoluminescence quantum efficiency of 54.6%) as a standard at room temperature.
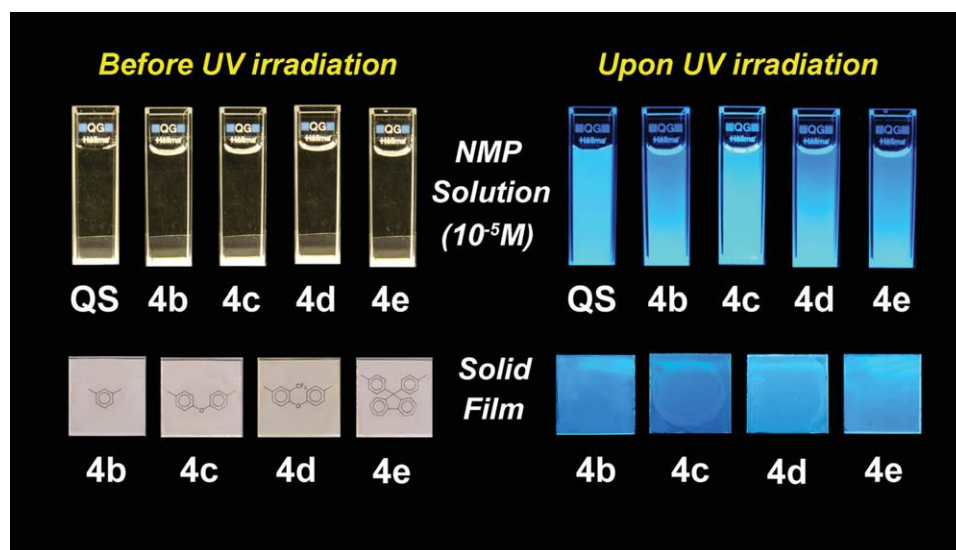
[e] Determined by cyclic voltammetry versus Ag/AgCl in acetonitrile.
[f] The data were calculated of thin film by the equation: E_g^{opt} (optical band gap) = 1240/λ_{onset} of polymer films.
[g] The HOMO energy levels were calculated from E_{onset} and were referenced to ferrocene (4.8 eV). $E_{LUMO} = E_{HOMO} - E_g^{opt}$.
[h] Irreversible oxidative process.

FIGURE 7 Photos of the solutions in NMP and solid films of the selected polyamides before and upon exposure to a standard laboratory UV lamp (Excited at 365 nm). Quinine sulfate (QS) dissolved in 1N H_2SO_4 (aq) (1 × 10^{-5} M) is used as a reference (Φ_F = 54.6%).

new broad absorption band around 703 nm started to intensify due to the cation radical formation. As shown in the inset of Figure 9, polyamide **4e** is almost colorless in the neutral state and pale blue in the oxidized state. Electrochromic switching studies were performed to monitor the absorbance changes as a function of time and to determine the switching time of the polymer at its absorption maximum by stepping potential repeatedly between the neutral and oxidized states. The switching time was defined as the time that was required to reach 90% of the full change in absorbance after switching potential because it is difficult to perceive any further color change with naked eye beyond this point. Thin films from polyamide **4e** would require 4.4 s at 1.35 V for reaching 90% absorbance at 703 nm and 2.7 s for bleaching. After several successive switchings between 0.0 and 1.35 V, the polymer films still exhibited fast response time and good redox and electrochromic stability (Fig. 10).

In addition, spectroelectrochemistry of polyamide **4f** was also investigated. As displayed in Figure 11, in the neutral form, at 0 V, the film exhibited strong absorption at wavelength around 366 nm due to π–π* transition of the polymer, but it was almost transparent in the visible region. Upon oxidation of the **4f** film (increasing applied voltage from 0 to 1.0 V), the intensity of the absorption peak at 366 nm gradually decreased while a new broadband having its maximum absorption wavelength at 805 nm gradually increased in intensity. We attribute this spectral change to the formation of a stable monocation radical originating from the oxidation of the amino center in the diamine residue of polymer **4f**. Further increase the applied electric potential to 1.55 V led to the drop of the absorption intensity at 805 nm with the concomitant increase of the intensity at 539 and 709 nm. This spectral change indicated the occurrence of the second oxidation arising from another TPA unit in the diacid component. The observed absorption changes in the film of **4f** at various potentials are fully reversible and are associated with strong color changes; indeed, they even can be seen readily by the naked eye. From the inset shown in Figure 11,

it can be seen that the film of **4f** switches from a transmissive neutral state (almost colorless) to a highly absorbing semioxidized state (green) and a fully oxidized state
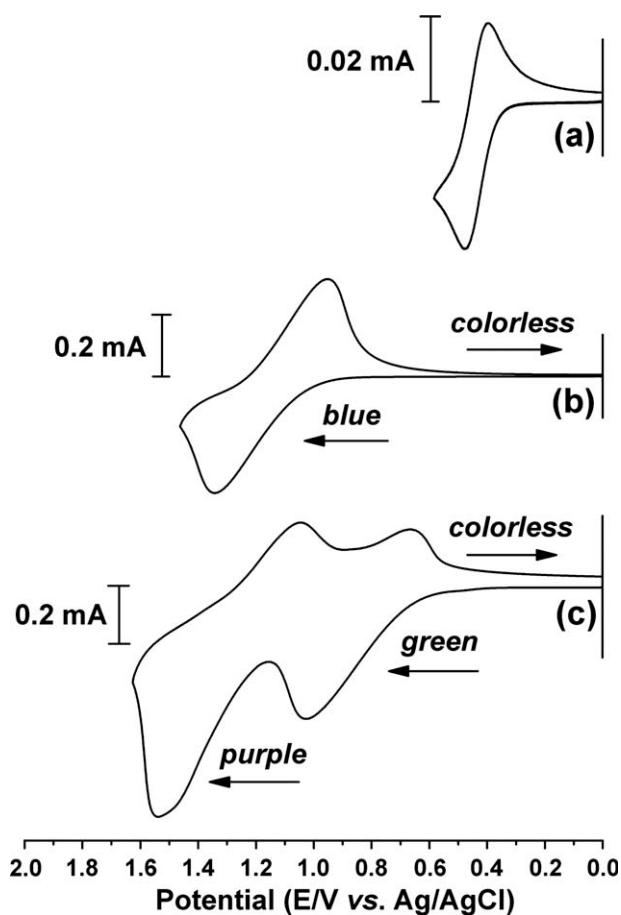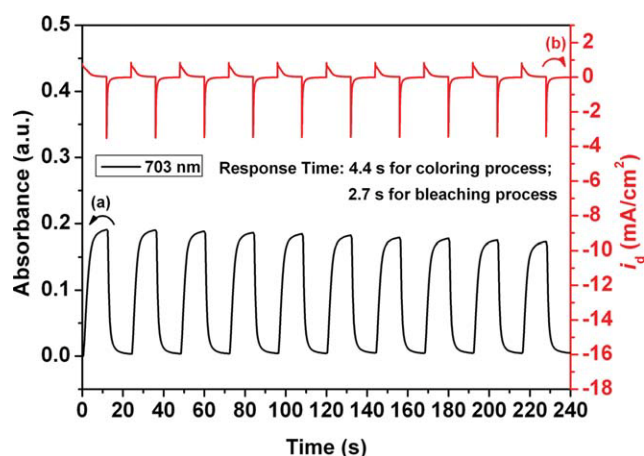

FIGURE 8 Cyclic voltammograms of (a) ferrocene, (b) polyamide **4e**, and (c) polyamide **4f** film on an ITO-coated glass substrate in the CH_3CN solution containing 0.1 M TBAP with a scan rate = 100 mV/s. The arrows indicate the film color change during scan.
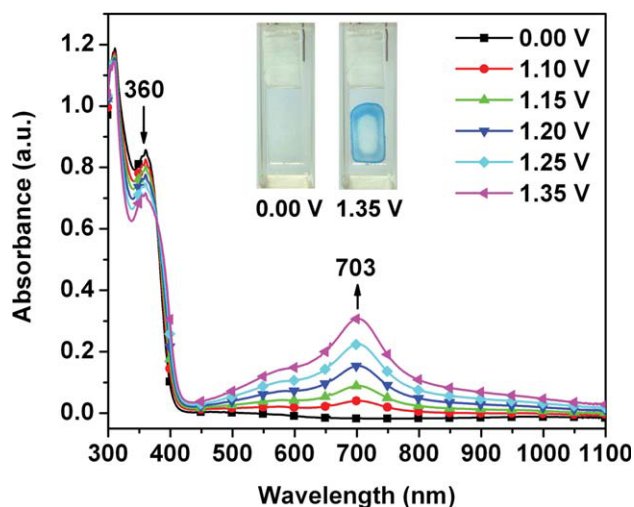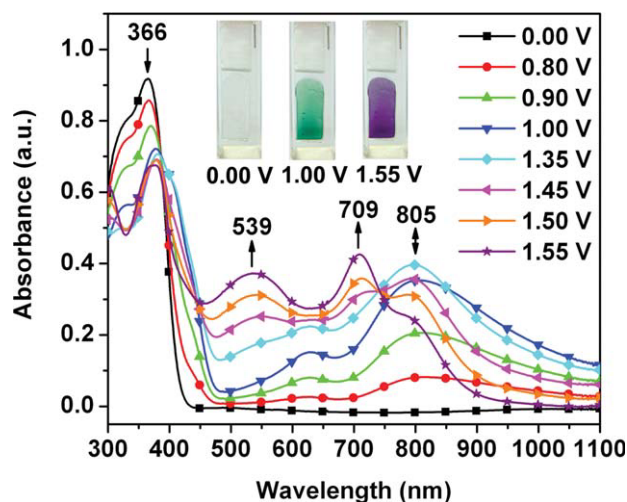
FIGURE 9 Spectral change of polyamide **4e** thin film on the ITO-coated glass substrate (in CH$_3$CN with 0.1 M TBAP as the supporting electrolyte) along with increasing of applied voltage (vs. Ag/AgCl couple as reference). The inset shows the photographic images of the film at indicated applied voltages. [Color figure can be viewed in the online issue, which is available at www.interscience.wiley.com.]

FIGURE 11 Spectral change of polyamide **4f** thin film on the ITO-coated glass substrate (in CH$_3$CN with 0.1 M TBAP as the supporting electrolyte) along with increasing of applied voltage (vs. Ag/AgCl couple as reference). The inset shows the photographic images of the film at indicated applied voltages. [Color figure can be viewed in the online issue, which is available at www.interscience.wiley.com.]

(purple). For optical switching studies, the polymer film of **4f** was cast on an ITO-coated glass slide, and the film was potential stepped between its neutral (0 V) and semioxidized (+1.0 V) state. While the potential was switched, the absorbance at 805 nm was monitored as a function of time. As depicted in Supporting Information Figure S5, thin film of polyamide **4f** required 3.1 s at 1.00 V for coloring and 2.1 s for bleaching. Switching data for the cast film of polyamide **4f** are given in Figure 12. The polyamides switch rapidly (within 4 s) between the highly transmissive neutral state

and the green colored oxidized state. Coloration efficiency (CE; η) was measured by monitoring the amount of ejected charge (Q) as a function of the change in optical density (ΔOD) of the polymer film. The electrochromic coloration efficiencies ($\eta = \Delta$OD$/Q$)[47,48] of the polymer films of **4f** after various switching cycles are summarized in Table 4. Coloration efficiency of **4f** was found to be 110 cm^2/C at 100% full switch at 805 nm. After 100 switching cycles between 0 V and 1.00 V, the film of polyamide **4f** only showed 4.5% decay on coloration efficiency. Therefore, the results of these
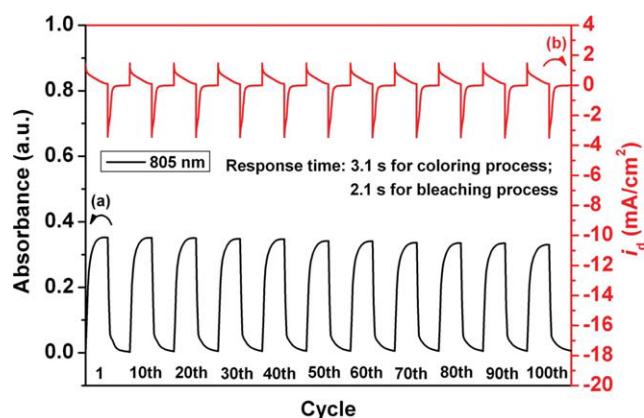

FIGURE 10 (a) Potential step absorptometry and (b) current consumption of the polyamide **4e** film on the ITO-coated glass substrate (active area ~1 cm^2) during the continuous cyclic test by switching potentials between 0 V and 1.35 V (vs. Ag/AgCl) with a cycle time of 24 s. [Color figure can be viewed in the online issue, which is available at www.interscience.wiley.com.]

FIGURE 12 (a) Potential step absorptometry and (b) current consumption of the polyamide **4f** film on the ITO-coated glass substrate (active area ~1 cm^2) during the continuous cyclic test by switching potentials between 0 V and 1.0 V (vs. Ag/AgCl) with a cycle time of 20 s. [Color figure can be viewed in the online issue, which is available at www.interscience.wiley.com.]

TABLE 4 Optical and Electrochemical Data Collected for the Coloration Efficiency Measurements of Polyamide **4f**

Switching Cycles[a]	ΔOD[b]	Q (mC/cm^2)[c]	η (cm^2/C)[d]	Decay (%)[e]
1	0.345	3.14	110	0.0
20	0.345	3.15	110	0.0
40	0.341	3.13	109	0.9
60	0.335	3.12	108	1.8
80	0.330	3.10	106	3.6
100	0.324	3.08	105	4.5

[a] Switching between 0 and 1.00 V (vs. Ag/AgCl).
[b] Optical density change at 805 nm.
[c] Ejected charge, determined from the *in situ* experiments.
[d] Coloration efficiency is calculated from the equation: $\eta = \Delta OD/Q$.
[e] Decay of coloration efficiency after various cyclic scans.

experiments revealed that the introduction of the *tert*-butyl group at the active sites of the TPA unit enhances the redox and electrochromic stability of these polymers.

CONCLUSIONS

A series of new polyamides **4a–f** with *tert*-butyl-substituted triphenylamine units were successfully prepared from 4-*tert*-butyl-4′,4″-dicarboxytriphenylamine and various aromatic diamines via the phosphorylation polyamidation reaction. The polyamides exhibit good solubility and film-forming capability and high thermal stability, and all of them are fluorescent with blue-light emission. The polymers display very well-defined and reversible redox processes in acetonitrile solutions. Furthermore, they possess electrochomic behavior. The polyamide **4f** containing the *tert*-butyltriphenylamine unit in both diacid and diamine components shows multi-electrochromic behavior: colorless in the neutral state, green in the semioxidized state, and purple in the fully oxidized state. Good redox and electrochromic stability, moderate fluorescence intensity, and proper HOMO values of these polyamides make them promising candidates for optoelectronic applications.

REFERENCES AND NOTES

1 Wienk, M. M.; Janssen, R. A. J. Chem Commun 1996, 267–268.

2 Selby, T. D.; Blackstock, S. C. Org Lett 1999, 13, 2053–2055.

3 Ito, A.; Ino, H.; Tanaka, K.; Kanemoto, K.; Kato, T. J Org Chem 2002, 67, 491–498.

4 Selby, T. D.; Kim, K.-Y.; Blackstock, S. C. Chem Mater 2002, 14, 1685–1690.

5 Murata, H.; Miyajima, D.; Nishide, H. Macromolecules, 2006, 39, 6331–6335.

6 Tang, C. W.; VanSlyke, S. A. Appl Phys Lett 1987, 51, 913–915.

7 Adachi, C.; Nagai, K.; Tamoto, N. Appl Phys Lett 1995, 66, 2679–2681.

8 Shirota, Y.; Okumoto, K.; Inada, H. Synth Met 2000, 111–112, 387–391.

9 Thelakkat, M. Macromol Mater Eng 2002, 287, 442–461.

10 Shirota, Y.; Kageyama, H. Chem Rev 2007, 107, 953–1010.

11 Liang, F.; Pu, Y.-J.; Kurata, T.; Kido, J. Nishide, H. Polymer , 2005, 46, 3767–3775.

12 Liang, F.; Kurata, T.; Nishide, H.; Kido, J. J Polym Sci Part A Polym Chem 2005, 43, 5765–5773.

13 Tang, R.; Tan, Z.; Li, Y.; Xi, F. Chem Mater 2006, 18, 1053–1061.

14 Kim, Y.-H.; Zhao, Q.; Kwon, S.-K. J Polym Sci Part A Polym Chem 2006, 44, 172–182.

15 Zhao, Q.; Kim, Y.-H.; Dang, T. T. M.; Shin, D.-C.; You, H.; Kwon, S.-K. J Polym Sci Part A Polym Chem 2007, 45, 341–347.

16 Su, H.-J.; Wu, F.-I.; Tseng, Y.-H.; Shu, C.-F. Adv Funct Mater 2005, 15, 1209–1216.

17 Wu, F.-I.; Yang, X.-H.; Neher, D.; Dodda, R.; Tseng, Y.-H.; Shu, C.-F. Adv Funct Mater 2007, 17, 1085–1092.

18 Wu, F.-I.; Shih, P.-I.; Tseng, Y.-H.; Shu, C.-F.; Tung, Y.-L.; Chi, Y. J Mater Chem 2007, 17, 167–173.

19 Mikroyannidis, J. A.; Gibbons, K. M.; Kulkarni, A. P.; Jenekhe, S. A. Macromolecules 2008, 41, 663–674.

20 Li, Y.; Xue, L.; Xia, H.; Xu, B.; Wen, S.; Tian, W. J Polym Sci Part A Polym Chem 2008, 46, 3970–3984.

21 Vellis, P. D.; Mikroyannidis, J. A.; Cho, M. J.; Choi, D. H. J Polym Sci Part A Polym Chem 2008, 46, 5592–5603.

22 Park, M. H.; Huh, J. O.; Do, Y.; Lee, M. H. J Polym Sci Part A Polym Chem 2008, 46, 5816–5825.

23 Hsieh, B.-Y.; Chen, Y. J Polym Sci Part A Polym Chem 2009, 47, 1553–1566.

24 Jiang, Z.; Zhang, W.; Yao, H.; Yang, C.; Cao, Y.; Qin, J.; Yu, G.; Liu, Y. J Polym Sci Part A Polym Chem 2009, 47, 3651–3661.

25 Sim, J. H.; Kim, S. J.; Yamada, K.; Yokokyra, S.; Natori, I.; Natori, S.; Sato, H. Synth Met 2009, 159, 85–90.

26 Park, M. H.; Yun, C.; Park, M. H.; Do, Y.; Yoo, S.; Lee, M. H. Macromolecules 2009, 42, 6840–6843.

27 Cassidy, P. E. Thermally Stable Polymers; Marcel Dekker: New York, 1980.

28 Yang, H. H. Aromatic High-Strength Fibers; Wiley: New York, 1989.

29 Oishi, Y.; Takado, H.; Yoneyama, M.; Kakimoto, M.; Imai, Y. J Polym Sci Part A: Polym Chem 1990, 28, 1763–1769.

30 Liou, G.-S.; Hsiao, S.-H.; Ishida, M.; Kakimoto, M.; Imai, Y. J Polym Sci Part A: Polym Chem 2002, 40, 2810–2818.

31 Liou, G.-S.; Hsiao, S.-H. J Polym Sci Part A: Polym Chem 2003, 41, 94–105.

32 Su, T.-H.; Hsiao, S.-H.; Liou, G.-S. J Polym Sci Part A: Polym Chem 2005, 43, 2085–2098.

33 Liou, G.-S.; Hsiao, S.-H.; Su, T.-H. J Mater Chem 2005, 15, 1812–1820.

34 Hsiao, S.-H.; Chang, Y.-M.; Chen, H.-W.; Liou, G.-S. J Polym Sci Part A: Polym Chem 2006, 44, 4579–4592.

35 Liou, G.-S.; Huang, N.-K.; Yang, Y.-L. Polymer 2006, 47, 7013–7020.

36 Chang, C.-W.; Liou, G.-S.; Hsiao, S.-H. J Mater Chem 2007, 17, 1007–1015.

37 Hsiao, S.-H.; Liou, G.-S.; Kung, Y.-C.; Yen, H.-J. Macromolecules 2008, 41, 2800–2808.

38 Chang, C.-W.; Yen, H.-J.; Huang, K.-Y.; Yeh, J.-M.; Liou, G.-S. J Polym Sci Part A: Polym Chem 2008, 46, 7937–7949.

39 Lin, H.-Y.; Liou, G.-S. J Polym Sci Part A: Polym Chem 2009, 47, 285–294.

40 Liou, G.-S.; Lin, K.–H. J Polym Sci Part A: Polym Chem 2009, 47, 1988–2001.

41 Hsiao, S.-H.; Liou, G.-S.; Wang, H.-M. J Polym Sci Part A: Polym Chem 2009, 47, 2330–2343.

42 Yen, H.-J.; Liou, G.-S. Chem Mater 2009, 21, 4062–4070.

43 Yang, C.-P.; Chen, R.-S.; Chen, K.-H. Colloid Polym Sci 2003, 281, 505–515.

44 Yamazaki, N.; Matsumoto, M.; Higashi, F. J Polym Sci Part A: Polym Chem 1975, 13, 1373–1380.

45 Demas, J. N.; Crosby, G. A. J Phys Chem 1971, 75, 991–1024.

46 Yan, H.; Huang, Q.; Cui, J.; Veinot, G. C.; Kern, M. M.; Marks, T. J. Adv Mater 2003, 15, 835–838.

47 Monk, P. M. S.; Mortimer, R. J.; Rosseinsky, D. R. Electrochromism and Electrochromic Devices, Cambridge University Press: UK, 2007.

48 Beaujuge, P. M.; Reynolds, J. R. Chem Rev 2010, 110, 268–320.